

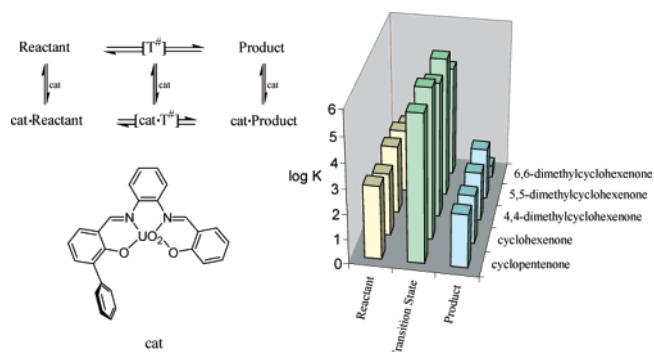
A Kinetic Study of the Conjugate Addition of Benzenethiol to Cyclic Enones Catalyzed by a Nonsymmetrical Uranyl–Salophen Complex

Valeria van Axel Castelli, Antonella Dalla Cort, Luigi Mandolini,* Valentina Pinto, and Luca Schiaffino

Dipartimento di Chimica and IMC-CNR, Università La Sapienza, 00185 Roma, Italy

luigi.mandolini@uniroma1.it

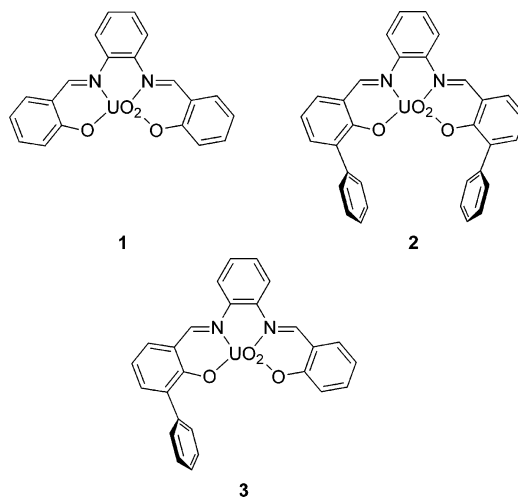
Received February 28, 2007



The Et₃N-assisted addition of benzenethiol to enones in chloroform is catalyzed with high turnover efficiency by the phenyl-substituted uranyl–salophen compound **3**. Catalytic data show a close adherence to a quaternary mechanism involving reaction of a base-activated thiol with a reversibly formed complex of enone and metal catalyst, with a complication of product inhibition due to the formation of a product–catalyst complex. The role of the binding energy made available by interactions with the aromatic sidearm of the catalyst is discussed in terms of catalyst–substrate and catalyst–transition state complementarity.

Salophen ligands (salophen = *N,N'*-phenylene salicylidene) are widely studied in coordination chemistry and have found application in supramolecular chemistry owing to the easy synthetic accessibility of a large variety of different structures.¹ In their robust complexes with the uranyl dication UO₂²⁺, the N₂O₂ donor atoms occupy four of the five coordination sites of the uranium, while leaving the fifth position available for labile coordination of a monodentate ligand.² Such Lewis acid–base interaction provides the basis for the use of

uranyl–salophen compounds as metalloreceptors³ and metal-locatalysts.⁴



Conjugate additions of thiols to activated olefins are biologically relevant⁵ and synthetically useful⁶ reactions. We reported that uranyl–salophen compounds **1** and **2** catalyze with high turnover efficiency the tertiary amine assisted addition of benzenethiol to cyclic and acyclic enones and provided a detailed description of the complex kinetics.^{4a–c}

The almost parallel pendants in **2** form a narrow cleft easily accessible by sterically unhindered, planar donor guests.⁷ Attractive van der Waals interactions of the guest with the cleft walls enhance complex formation.^{3b} Association constants (Table 1) with a number of enones (**4a–8a**) and their phenylthio

(3) (a) Antonisse, M. M. G.; Reinhoudt, D. N. *Chem. Commun.* **1998**, 443–448. (b) van Axel Castelli, V.; Dalla Cort, A.; Mandolini, L.; Pinto, V.; Reinhoudt, D. N.; Ribaud, F.; Sanna, C.; Schiaffino, L.; Snellink-Ruël, B. H. M. *Supramol. Chem.* **2002**, *14*, 211–219. (c) Dalla Cort, A.; Miranda Murua, J. I.; Pasquini, C.; Pons, M.; Schiaffino, L. *Chem.–Eur. J.* **2004**, *10*, 3301–3307. (d) Cametti, M.; Nissinen, M.; Dalla Cort, A.; Mandolini, L.; Rissanen, K. *J. Am. Chem. Soc.* **2005**, *127*, 3831–3837. (e) Cametti, M.; Nissinen, M.; Dalla Cort, A.; Mandolini, L.; Rissanen, K. *J. Am. Chem. Soc.* **2007**, *129*, 3641–3648.

(4) (a) van Axel Castelli, V.; Dalla Cort, A.; Mandolini, L.; Reinhoudt, D. N. *J. Am. Chem. Soc.* **1998**, *120*, 12688–12689. (b) van Axel Castelli, V.; Dalla Cort, A.; Mandolini, L.; Reinhoudt, D. N.; Schiaffino, L. *Chem.–Eur. J.* **2000**, *6*, 1193–1198. (c) van Axel Castelli, V.; Dalla Cort, A.; Mandolini, L.; Reinhoudt, D. N.; Schiaffino, L. *Eur. J. Org. Chem.* **2003**, 627–633. (d) Dalla Cort, A.; Mandolini, L.; Schiaffino, L. *Chem. Commun.* **2005**, 3867–3869.

(5) (a) Fluharty, A. L. In *The Chemistry of the Thiol Group*, Part 2; Patai, S., Ed.; Wiley: New York, 1974; p 589. (b) Jocelyn, P. C. In *Biochemistry of the SH Group*; Academic Press: London, 1972; p 98. For recent examples, see: (c) Lutolf, M.P.; Tirelli, N.; Cerritelli, S.; Colussi, L.; Hubbell, J. *Bioconjugate Chem.* **2001**, *12*, 1051–1056. (d) Schmidt, T. J.; Ak, M.; Mrowietz, U. *Bioorg. Med. Chem.* **2007**, *15*, 333–342.

(6) For selected examples, see: (a) Adam, W.; Nava-Salgado, V. O. *J. Org. Chem.* **1995**, *60*, 578–584. (b) Michael, K.; Kessler, H. *Tetrahedron Lett.* **1996**, *37*, 3453–3456. (c) Sreekumar, R.; Rugmini, P.; Padma Kumar, R. *Tetrahedron Lett.* **1997**, *38*, 6557–6560. (d) Rohrig, S.; Hennig, L.; Findesein, M.; Welzel, P.; Frischmuth, K.; Marx, A.; Petronisch, T.; Koll, P.; Müller, D.; Mayer-Figge, H.; Sheldrich, W. S. *Tetrahedron* **1998**, *54*, 3413–3438. (e) Cheng, S.; Comer, D. D. *Tetrahedron Lett.* **2002**, *43*, 1179–1181. (f) Heggli, M.; Tirelli, N.; Zisch, A.; Hubbell, J. A. *Bioconjugate Chem.* **2003**, *14*, 967–973. (g) McDaid, P.; Chen, Y.; Deng, L. *Angew. Chem., Int. Ed.* **2002**, *41*, 338–340.

(7) Van Doorn, A. R.; Bos, M.; Harkema, S.; Van Eerden, J.; Verboom, W.; Reinhoudt, D. N. *J. Org. Chem.* **1991**, *56*, 2371–2380.

* To whom correspondence should be addressed. Tel: +39 0649913624. Fax: +39 06490421.

(1) Vigato, P. A.; Tamburini, S. *Coord. Chem. Rev.* **2004**, *248*, 1717–2128.

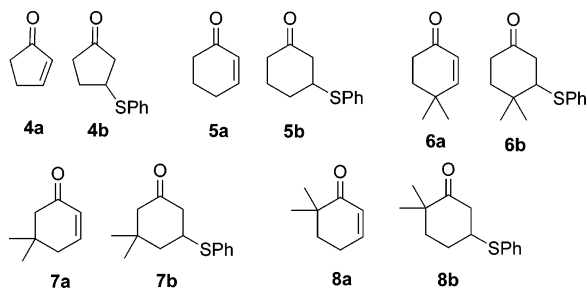
(2) (a) Sessler, J. L.; Melfi, P. J.; Pantos, G. D. *Coord. Chem. Rev.* **2006**, *250*, 816–843. (b) Ephritikhine, M. *Dalton Trans.* **2006**, 2501–2516.

TABLE 1. Association Constants for Complexes between Salophen–Uranyl Receptors 1–3 and Carbonyl Compounds 4–8 in CHCl_3 at 25.0 °C^a

	1	2	3
4a	14 ± 1	460 ± 40	870 ± 120
4b	<3	68 ± 6	140 ± 20
5a	7.6 ± 0.6	900 ± 200	320 ± 50
5b	<3	100 ± 20	90 ± 20
6a	17 ± 2	820 ± 150	530 ± 80
6b	<3	240 ± 20	90 ± 10 ^b
7a	3.7 ± 1.2	130 ± 20	330 ± 40
7b	<3	70 ± 7	110 ± 10 ^b
8a	3.2 ± 0.4	6.4 ± 1.4	90 ± 8
8b	<3	<3	<3 ^b

^a Data from refs 3b and 4a, unless otherwise stated. ^b This work, from UV–vis titrations.

derivatives (**4b–8b**) exceed those obtained with the parent compound **1** by 1–2 orders of magnitude, with the notable exception of the 6,6-dimethyl derivatives **8a** and **8b**, in which the bulky *gem*-dimethyl group apparently hinders effective insertion of the guest into the narrow cleft.



Our interest in nonsymmetrically substituted uranyl–salophen derivatives⁸ led us to the discovery that van der Waals interactions of the bound substrates with the single aromatic sidearm in **3** are strong enough to ensure binding affinities comparable to those of the complexes with **2** (Table 1). Again the 6,6-dimethyl derivative **8a** is an exception, in that its binding affinity to **3** is much higher than to **2**. It was felt therefore that the “half-cleft” receptor **3** could act as a catalyst of the conjugate thiol addition to enones, capable of combining the advantages of compounds **1** and **2**, because it binds to the enone substrate with affinities comparable or even greater than those of **2**, while leaving one of the two faces of the activated double bond more accessible to nucleophile addition. With this idea in mind, we have carried out a careful kinetic study of the conjugate addition of benzenethiol to enones **4a–8a** in chloroform solution, catalyzed by a combination of triethylamine and compound **3**.

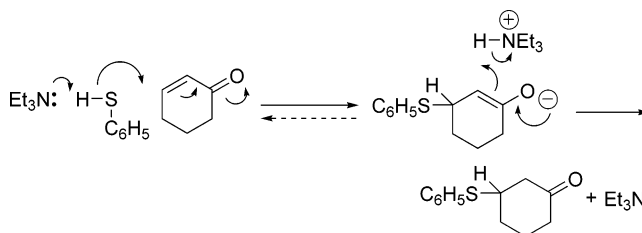
As shown in a previous study,^{4c} the rate law for the tertiary amine (B) catalyzed addition of benzenethiol (T) to enones (E) is that of a clean third-order process (eq 1).

$$\text{rate} = k_0[\text{B}][\text{T}][\text{E}] \quad (1)$$

Since the concentration of the base catalyst is constant in a given run, second-order time dependence was actually observed, with $k_{\text{obs}} = k_0[\text{B}]$. Consistent with the kinetics, the reaction mechanism is depicted as a termolecular process (Scheme 1),

(8) For a review article, see: Dalla Cort, A.; Pasquini, C.; Schiaffino, L. *Supramol. Chem.* **2007**, *19*, 79–87.

SCHEME 1. Mechanism of the Conjugate Addition of Benzenethiol to Enones in Nonpolar Solvents



which does not necessarily imply a three-body collision, but can instead be accomplished by the reaction of the enone with a weak complex of thiol and base. In the mechanism depicted in Scheme 1, a proton is first transferred from sulfur to nitrogen, and then from nitrogen to the α -carbon atom of the enolate intermediate. The kinetics reveal the composition of the rate-limiting transition state as that of a ternary complex of base, thiol, and enone in a 1:1:1 ratio, but is uncertain whether it is the formation or disruption of the BH^+ -paired enolate that is rate determining. The rate constants k_0 for the Et_3N -catalyzed addition of benzenethiol to enones **4a–8a** listed in the first column in Table 2 show that, within the cyclohexenone series, the reaction is quite sensitive to the presence of the bulky *gem*-dimethyl group and to its distance from the site of nucleophilic attack.^{4b}

Addition of catalytic amounts of metal catalyst **3** strongly enhances rates of addition of benzenethiol to enones **4a–8a**. Typical time–concentration data from ^1H NMR analysis of the reaction mixtures are plotted in Figure 1. In all cases, the disappearance of the enone reactant was complete and was accompanied by the equivalent formation of the addition product. No extra peaks due to reaction intermediate and/or side products were observed.

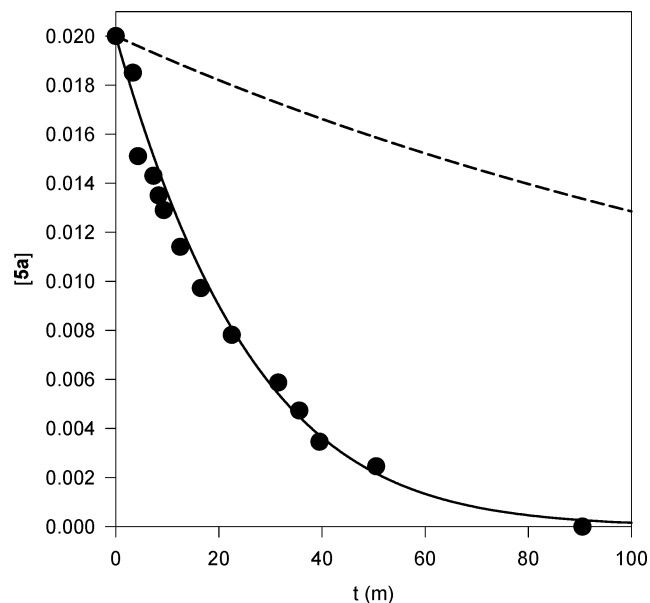


FIGURE 1. Time–concentration profile for the Michael type addition of 0.05 M benzenethiol to 0.02 M **5a** in the presence of 1 mM Et_3N and 0.1 mM **3**. The points are obtained from ^1H NMR analysis, and the solid line is calculated from eq 3. The dotted line is the time–concentration profile for the same reaction in the absence of metal catalyst calculated from the k_0 value in Table 2.

TABLE 2. Kinetic Data for the Addition of Benzenethiol to Enones 4a–8a in the Presence of Et₃N and in the Absence (*k*_o) and Presence (*k*_{cat}) of Metallocatalysts 1–3 in CHCl₃ at 25.0 °C^a

	1					2				3			
	<i>k</i> _o	<i>k</i> _{cat}	<i>k</i> _{cat} / <i>k</i> _o	<i>k</i> _{cat} <i>K</i> _E	<i>K</i> _{T‡}	<i>k</i> _{cat}	<i>k</i> _{cat} / <i>k</i> _o	<i>k</i> _{cat} <i>K</i> _E	<i>K</i> _{T‡}	<i>k</i> _{cat} ^b	<i>k</i> _{cat} / <i>k</i> _o	<i>k</i> _{cat} <i>K</i> _E	<i>K</i> _{T‡}
4	1.6	1400	880	2.0 × 10 ⁴	1.2 × 10 ⁴	630	390	2.9 × 10 ⁵	1.8 × 10 ⁵	1300	810	1.1 × 10 ⁶	7.1 × 10 ⁵
5	0.66	1600	2400	1.2 × 10 ⁴	1.8 × 10 ⁴	710	1100	6.4 × 10 ⁵	9.7 × 10 ⁵	2700	4100	8.6 × 10 ⁵	1.3 × 10 ⁶
6	0.024	10	420	170	7.0 × 10 ³	1.8	75	1500	6.2 × 10 ⁴	11	460	5800	2.4 × 10 ⁵
7	0.080	320	4000	1200	1.5 × 10 ⁴	100	1200	1.3 × 10 ⁴	1.6 × 10 ⁵	90	1100	2.9 × 10 ⁴	3.6 × 10 ⁵
8	0.14	480	3400	1500	1.1 × 10 ⁴	2.6	19	17	120	40	290	3600	2.6 × 10 ⁴

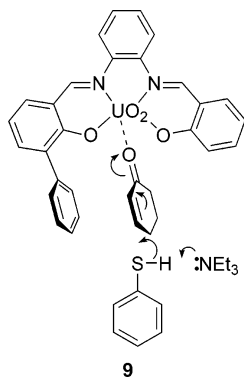
^a All quantities are defined in eqs 1 and 2. Rate constants *k*_o and *k*_{cat} have units of M⁻² s⁻¹; equilibrium constants *K*_E and *K*_{T‡} [*K*_{T‡} = (*k*_{cat}/*k*_o)·*K*_E] have units of M⁻¹. Rate constants *k*_o and catalytic constants *k*_{cat} for reactions catalyzed by 1 and 2 from refs 4a–c. Equilibrium constants *K*_E from Table 1. ^b Experimental errors calculated as ± 2σ (95% confidence limit) are in the order of ± 5%.

As previously found for the reactions catalyzed by 1 and 2,^{4b} in the presence of 3, the reactions no longer exhibited second-order time dependence because the metal catalyst 3 binds significantly to the enone reactant and, in the majority of cases, also to the reaction product. The bound enone plays a key role in the catalysis, as interaction with the Lewis acidic uranyl center strongly stabilizes the negative charge transferred from the sulfur nucleophile to the carbonyl oxygen. The proposed mechanism (Scheme 2) is an extended complexation catalysis scheme,

SCHEME 2. Complexation Catalysis with Product Inhibition in the Conjugate Addition of Benzenethiol to Enones in Nonpolar Solvent in the Presence of Uranyl–Salophen Catalyst (cat)



involving a combination of Brønsted base (B) and Lewis acid (cat) catalysts and product inhibition caused by the formation of a product–catalyst complex (P-cat). The highest energy transition state has the composition of a quaternuclear complex (9) arising from the addition of a base-activated thiol to an enone–catalyst complex.



Whenever the rate of the reaction catalyzed by the base alone is significant compared with the rate of the reaction catalyzed by a combination of base and metal catalyst, the overall reaction rate is given by eq 2, where the second term on the right is a direct consequence of Scheme 2 and holds whenever [E·cat] ≪ [E]. Analytical integration of eq 2 has been reported previously.^{4b,c} The form that the integrated equation takes for the case of unequal reactant concentrations is that of eq 3, where the quantities *m* and *n* are defined in eqs 4 and 5, respectively. This is an unpleasantly complicated equation, but its practical application is straightforward.

$$\text{rate} = k_o[B][T][E] + \frac{k_{\text{cat}}K_E[B][T][E][\text{cat}]_{\text{tot}}}{1 + K_E[E] + K_P[P]} \quad (2)$$

Numerical values of the quantities *k*_o (Table 2), *K*_E, and *K*_P (Table 1) are known from independent measurements, and the composition of the reaction mixtures as a function of time is known from ¹H NMR data. Hence the only unknown quantity is *k*_{cat}. For each catalytic run, a value of *k*_{cat} was chosen in such a way that the left side of eq 3 plots against time as a straight line through the origin with slope 1. An example of such plots is shown in Figure 2, based on the time–concentration data in Figure 1. In all cases, time–concentration profiles were reproduced to a good precision upon introduction of the optimized *k*_{cat} value into eq 3. It is significant that a good adherence of data points to eq 3 was obtained using *K*_E and *K*_P values from independent measurements and not merely by a fitting procedure in which such quantities are treated as adjustable parameters.

$$\frac{1 + K_P[E]_o}{m([T]_o - [E]_o)} \ln \frac{[E]_o}{[E]} + \left(\frac{K_E - K_P}{m - n} - \frac{1 + K_P[E]_o}{(m - n)([T]_o - [E]_o)} \right) \ln \frac{[T]_o}{[T]} + \frac{(K_E - K_P)k_{\text{cat}}K_E[B][\text{cat}]_{\text{tot}}}{m(m - n)} \ln \left(1 - \frac{(K_E - K_P)k_o([E]_o - [E])}{k_o + k_{\text{cat}}K_E[\text{cat}]_{\text{tot}} + k_oK_E[E]_o} \right) = t \quad (3)$$

$$m = k_o[B](1 + K_P[E]_o) + k_{\text{cat}}K_E[B][\text{cat}]_{\text{tot}} \quad (4)$$

$$n = k_o[B]([T]_o - [E]_o)(K_P - K_E) \quad (5)$$

The kinetic parameters for the reactions catalyzed by 3 are summarized in Table 2, where the corresponding data for the reactions catalyzed by 1 and 2 are also reported for comparison. Like in the simple Michaelis–Menten mechanism of enzyme kinetics,⁹ the relevant parameters are *k*_{cat} and *k*_{cat}·*K*_E. The meaning of *k*_{cat} is that of the rate constant for the transformation of the catalyst-bound enone into the catalyst-bound product, with the obvious difference that here *k*_{cat} is a third-order rate constant not first order as in the Michaelis–Menten kinetics. The quantity *k*_{cat}·*K*_E is an apparent fourth-order rate constant that refers to the properties and reaction of the free catalyst and free substrate

(9) Fersht, A. In *Enzyme Structure and Mechanism*, 2nd ed.; W.H. Freeman: New York, 1985; Chapter 3.

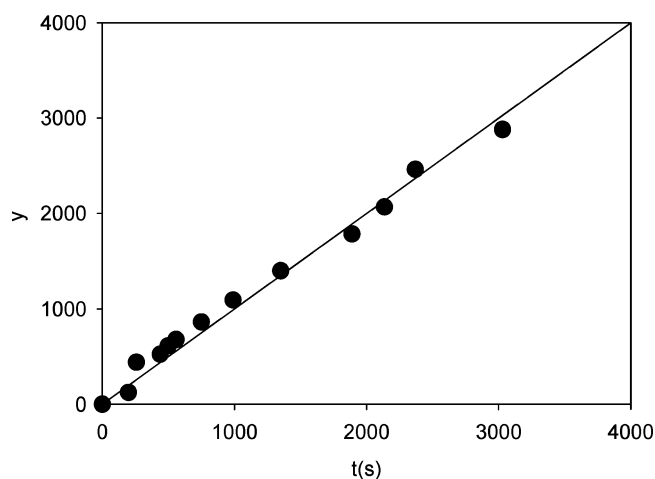


FIGURE 2. Plot of the left side of eq 3 against time for the addition of benzenethiol to 2-cyclohexen-1-one **5a** in the presence of Et₃N and **3**, with $k_{\text{cat}} = 2700 \text{ M}^{-2} \text{ s}^{-1}$. The straight line has a slope of 1.

(subsaturating conditions), and that determines the selectivity for competing substrates at any substrate concentration. The dimensionless quantity k_{cat}/k_0 is a quantitative measure of the increase of substrate reactivity upon complexation with the uranyl catalyst, whereas the product $(k_{\text{cat}}/k_0) \cdot K_{\text{E}}$ defines the equilibrium constant K_{T^\ddagger} for the transformation of the transition state T^\ddagger into the catalyst–transition state complex $\text{cat} \cdot \text{T}^\ddagger$.¹⁰

In line with expectations, the aromatic sidearm in **3** contributes significantly to the binding of the transition states in all cases, as shown by the fact that the K_{T^\ddagger} values are the highest for the reactions catalyzed by **3** (Table 2). In the reactions of enones **4a–6a**, catalysts **1** and **3** show very similar k_{cat} values, in spite of the much higher affinity of catalyst **3** toward the transition states of the given reactions. This is a consequence of the fact that the additional binding energy rendered available by the van der Waals interactions with the aromatic pendant in **3** is realized equally well in the catalyst–enone complex and in the catalyst–transition state complex, so that the free energies are lowered by very nearly the same amounts. In the language of Fersht, there is both catalyst–substrate and catalyst–transition state complementarity.¹¹ Only in dilute substrate solutions (i.e., $K_{\text{E}} \cdot [\text{E}] \ll 1$) will catalyst **3** perform much more effectively than **1** because the sole factor at work is stabilization of the transition state and not the differential stabilization of transition and reactant states.

Interestingly, in the reactions of enones **4a–6a**, the k_{cat} values measured in the presence of **3** are larger than those measured in the presence of **2**, which indicates that the binding energy made available by the cleft walls in **2** is realized more effectively in the reactant state than in the transition state. In the reaction of enone **7a**, catalysts **2** and **3** perform much in the same way, about 3 times less effectively than catalyst **1**, showing that a *gem*-dimethyl group in position 5 has only a moderately adverse

effect on catalyst–transition state complementarity. Markedly different behaviors, however, are observed in the reactions of enone **8**. Here the *gem*-dimethyl group in position 6 reduces dramatically the catalyst–transition state complementarity in the case of **2**, but much less so in the case of **3**. The net result is that k_{cat} for the reaction of **3** is still $1/12$ that of **1**, but well 15-fold higher than that of **2**. The single sidearm in **3** shows a better transition state complementarity than the two sidearms in **2** because the former can accommodate sterically hindered transition states.

To sum up, like its congeners **1** and **2**, uranyl–salophen complex **3** binds reversibly to enones **4a–8a** and promotes reactions of the bound substrates. The higher stability of the catalyst complexes of the enone reactants compared with those of the addition products ensures effective turnover catalysis with low product inhibition. A major driving force for catalysis, the only one in the case of **1**, is provided by interaction of the uranyl center with the carbonyl oxygen of the altered enone in the transition state (dynamic binding).¹² The passive binding¹² due to van der Waals interactions with the aromatic sidearm in **3** is realized both in the transition state and in the reactant state. Consequently, **3** is a far superior catalyst to **1** only under subsaturating conditions, but shows either comparable or lower catalytic activity under conditions approaching saturation. In line with expectations, the more open structure of the half-cleft catalyst **3** compared with that of metallocleft **2** makes the reactions catalyzed by the former much less sensitive to the adverse influence of steric effects.

Experimental Section

Instruments and Methods. ¹H NMR spectra were recorded in CDCl₃ with either a 200 or 300 MHz spectrometer. Association constants of **6b–8b** with **3** were determined spectrophotometrically at 430 nm according to standard titration procedures.^{3b}

Materials. Benzenethiol was distilled under reduced pressure prior to use. Triethylamine was distilled over *p*-toluenesulfonyl chloride and then over sodium. Spectrophotometric grade chloroform and chloroform-*d*₁ were dried over 4 Å molecular sieves for at least 24 h prior to use. Enones **4a**, **5a**, and **6a** were used as received. Compounds **7a**, **8a**, **6b**, **7b**, **8b**, and uranyl–salophen complex **3** were available from previous works.^{3b,4b}

Rate Measurements. NMR tubes were dried in an oven at 130 °C for at least 24 h and then stored in a desiccator. All sample manipulations were carried out under an argon atmosphere. Calculated amounts of triphenylmethane (internal standard) and of all of the reactants except triethylamine were introduced into an NMR tube, and a spectrum (either at 200 or 300 MHz, $T = 25.0$ °C) was recorded at time zero. Then a known amount of triethylamine was added, and spectra were recorded at selected time intervals. The integral of the signal of the α proton of the double bond of the enone was compared with that of the internal standard. Time–concentration data were fitted to eq 3. Because of the mathematical form of this equation, the enone concentration was taken as the independent variable in the curve-fitting procedure.

Acknowledgment. We acknowledge MIUR, COFIN 2003, Progetto Dispositivi Supramolecolari for financial contribution.

JO070357M

(10) Kurz, J. L. *J. Am. Chem. Soc.* **1963**, *85*, 987–991.

(11) Fersht, A. In *Enzyme Structure and Mechanism*, 2nd ed.; W.H. Freeman: New York, 1985; Chapter 12.

(12) Kirby, A. J. *Angew. Chem., Int. Ed. Engl.* **1996**, *35*, 706–724.